ASSESSMENT OF GEOMETRIC VARIABILITY EFFECTS THROUGH A VISCOUS THROUGH-FLOW MODEL APPLIED TO MODERN AXIAL-FLOW COMPRESSOR BLADES

A. Budo[1*], *K. Hillewaert*[1], *J. Bartholet*[2] *and V. E. Terrapon*[1]

[1] University of Liège, Aerospace and Mechanical Engineering, Allée de la Découverte 9, 4000 Liege, Belgium; arnaud.budo@uliege.be (*Correspondence), koen.hillewaert@uliege.be, vincent.terrapon@uliege.be

[2] Safran Aero Boosters, Aerodynamics Engineering Department, Route de Liers 121, 4041 Herstal (Milmort), Belgium; jules.bartholet@safrangroup.com

ABSTRACT

The overall goal of the present study is to evaluate the adequacy of a viscous time-marching through-flow solver to predict geometric variability effects on compressor performance. Although the computational efficiency of such a low-fidelity solver is useful for parametric studies, it is known that the involved assumptions and approximations associated with the through-flow (TF) approach introduce errors in the performance prediction. Thus, we first evaluate the model with respect to its underlying assumptions and correlations. To do so, TF simulations are compared to RANS simulations applied to a modern low-pressure compressor designed by Safran Aero Boosters. On the one hand, the TF simulations are fed with the exact radial distribution of the correlation parameters using RANS input data in order to isolate the modeling error from correlation empiricism. On the other hand, correlations from the literature are assessed and improved. Then, two modeling aspects linked to the blade leading edge, namely the incidence correction and the camber line computation, are discussed. As geometric variability precisely at the blade leading edge has a significant impact on the performance, we assess how these two aspects influence the variability propagation in this region. Moreover, we propose a strategy to mitigate these model uncertainties. Finally, geometric variabilities are introduced at the blade leading edge and the resulting variation in performance is quantified. It is shown that the solver provides realistic predictions of performance but is highly sensitive to the underlying correlations.

KEYWORDS

Viscous through-flow model, subsonic axial compressor, 3D blades, geometric variability RANS

NOMENCLATURE

x, r, θ	cylindrical coordinates
b	tangential blockage factor
f	body force
i	incidence angle
l	streamline length
$\dot{m}$	mass-flow rate
p	pressure
$\mathbf{S}$	source terms/body forces
s	entropy
t	blade thickness
T	temperature
V/W	velocity in the absolute/relative frame

Greek symbols

δ	deviation angle
κ	blade angle
ρ	density
Ω	rotation velocity of the shaft
ω	loss coefficient

Subscripts

b	blade force
c	cylindrical
i, v	inviscid/viscous
s	stress
t	total quantities

INTRODUCTION

The axial-flow compressor design is characterized by a constant search for the compromise between performance and manufacturing cost. The manufacturing tolerance of the blade, and in particular of its leading edge, is a good example: its shape has a high impact on aerodynamic performance whilst ensuring high geometric accuracy entails a severe manufacturing cost. Recent works (Nigro 2018, Lange et al. 2012) on this topic rely on Computational-Fluid-Dynamics (CFD) simulations to propagate variability of the geometry to that of performance. This approach is computationally expensive as the already non-negligible cost of a single simulation, generally based on the Reynolds-averaged Navier-Stokes (RANS) equations, is further compounded by the large number of simulations required. However, it is of utmost importance to be able to predict the effects of tolerances on the performance dispersion, within a time scale compatible with the design process. In this context, the computational efficiency of through-flow (TF) solvers is useful for parametric studies during design improvement phases in which many parameters or geometric variabilities are involved and robust design is targeted. It is however known that such an averaged two-dimensional CFD modeling approach is fundamentally limited in its ability to represent some turbomachinery flow features, due to the intrinsic limitations of the through-flow equations and the approximations and assumptions made in the closure models (Simon 2007). It is thus unclear whether the low computational cost of through-flow models can be leveraged for the practical quantification and propagation of geometric variability.

Specifically, a through-flow model, even based on Navier-Stokes (N-S) equations, cannot predict the prerotation of the flow upstream of a blade row due to the axisymmetry assumption on which the model is based (Baralon et al. 1998). In the analysis mode, the flow angles in the bladed region are imposed by a blade flow deflection force. Therefore, a discontinuity occurs at the leading edge if the flow incidence is not aligned with the mean blade camber. This discontinuity leads to a sudden and non-physical increase of entropy and a spurious loss generation. A common fix consists in modifying the blade angle in the leading-edge region so that it adapts to the incident flow. As a result, the blade geometry is locally modified by this numerical artifact; this modification can thereby smooth any impact of variabilities at the leading edge on the performance.

Furthermore, modern optimized airfoils are directly described by a distribution of points along the suction and pressure airfoil surface, unlike NACA airfoils which are parameterized classically based on a camberline/thickness distribution description; the latter is generally used for through-flow simulations. Therefore, the section outline splitting into mean camber line and thickness distribution has to be achieved through an inverse computation algorithm. However, in the vicinity of the leading edge (LE) and trailing edge (TE), algorithms determining a mean camber line can be unreliable (Lange et al. 2009). This epistemic uncertainty, although usually having a small impact, can still completely mask geometric variability in the leading edge region.

As geometric variability precisely near the blade leading edge has a significant impact on the performance, the overall goal is thus to determine through a sensitivity analysis how to represent these uncertainties in the through-flow model and how the modeling aspects impact their propagation. We consider subsonic viscous through-flow simulations of a modern highly loaded multi-stage axial low-pressure compressor. We first evaluate the through-flow model with respect to its underlying assumptions and correlations. In this context, we also propose several modifications of the correlations to improve the prediction. Then, the two modeling aspects related to the blade leading edge are discussed and strategies to mitigate these model uncertainties are proposed. Finally, geometric variabilities are introduced on the blade leading edge to assess the model ability to capture the resulting performance variability with respect to steady 3D RANS computations. The present analysis represents a first preliminary step in the overall study of geometric variabilities.

THROUGH-FLOW MODEL

Adamczyk cascade

The computational efficiency of through-flow methodologies stems from the pitch-wise averaged representation of the three-dimensional (3D) flow field in the meridional stream surface. However, this averaging process brings additional terms that are unclosed. Such a modeling approach has been used for decades in axial turbomachines and many different models with various levels of approximation have been developed over the years. They can be divided into two groups. The first is known as the streamline curvature (SLC) method (Wu 1952) and remains the backbone of the industrial compressor and turbine design process. The second type of through-flow models has been driven by the growth of computing power over the years. This approach, borrowed from traditional CFD methods, is mostly based on the pitch-wise averaged inviscid Euler equations (Pacciani et al. 2016, Righi et al. 2018, Föllner et al. 2020). Navier-Stokes-based through-flow models, such as the one used in the present study, have also been proposed occasionally (Simon 2007, Jian et al. 2020). Because all these models are based on different governing equations and closure models, which influence the level of empiricism and error, it is important for users and developers to know the underlying assumptions in order to characterize the associated modeling error. The Adamczyk's averaging cascade approach (Adamczyk 1984, Simon 2007) formalizes the different levels of CFD modeling encountered in numerical simulations by rigorously deriving a set of equations through a cascade of averages. The succession of four averages links the three-dimensional unsteady turbulent flow to a stationary axisymmetric meridional flow and defines the hierarchy of modeling levels. Specifically, it consists of an ensemble Reynolds averaging, a time-averaging, a passage-to-passage averaging and a circumferential averaging. The equations that are obtained for the averaged quantities are thus mathematically exact and help identifying in a rigorous and exhaustive manner the unclosed source terms.

These source terms can be divided into two categories. On the one hand, blade forces explicitly appear during the averaging process because the integration bounds of the averaging are not constant over the domain. These terms represent the forces exerted on the flow by the implicit presence of the blade in the two-dimensional meridional flow. They only apply in the region of the domain corresponding to the fictitious presence of the blade in the meridional plane. On the other hand, stresses appear due to the non-linearity of the Navier-Stokes equations. These terms represent the mean effects of the flow features that are eliminated by the averaging in the whole meridional plane. Simon (2007) showed that the results of through-flow simulations fed with the exact value of source terms from corresponding high-fidelity computations lead to quasi perfect match of performance prediction. However, these exact values are often elusive because the mathematical expression of unclosed terms depend on quantities that are not resolved by the through-flow solver. In practice, these terms are obtained from closure models or, for some, simply neglected. These simplifications and approximations inevitably result in errors.

Viscous through-flow equations

The viscous time-marching through-flow model used in the present analysis is based on the averaged Navier-Stokes equations. The blade body forces are implemented in the `ASTEC` code developed by Safran Tech and the authors. This software couples Onera's CFD solver `elsA` with its own routines to compute the axisymmetric N-S equations and solve the two-dimensional meridional flow. In this paper, the meridional problem is solved in the analysis mode as the performance for a known geometry is sought. The averaged equations in cylindrical coordinates (x, r, θ) read

$$\frac{\partial \mathbf{U}}{\partial t} + \frac{\partial \left(\mathbf{F_i} - \mathbf{F_v}\right)}{\partial x} + \frac{\partial \left(\mathbf{G_i} - \mathbf{G_v}\right)}{\partial r} = \mathbf{S}, \tag{1}$$

where x, r, θ are the stream-wise, span-wise and pitch-wise coordinates, $\mathbf{U}$ is the vector of transported variables, $\mathbf{F_i}$ and $\mathbf{G_i}$ the inviscid fluxes, $\mathbf{F_v}$ and $\mathbf{G_v}$ the viscous fluxes and $\mathbf{S}$ the sum of the source terms, respectively. The source terms contain the inviscid blade force $\mathbf{S_{bi}}$, the viscous blade force $\mathbf{S_{bv}}$, stresses $\mathbf{S_s}$ and miscellaneous terms originating in the evaluation of the flux divergence in cylindrical coordinates. Finally, blockage factor dependent terms are also included in $\mathbf{S}$. They stem from the expansion of the partial derivatives of the left-hand side to eliminate the blockage factor b from the fluxes. As a reminder, the blockage factor accounts for the blade thickness inside the channel in the definition of the averaging operator. Note that the aforementioned miscellaneous and blockage factor terms do not need closure. The detailed set of equations associated with Eq. 1 can be found in Budo et al. (2021).

Closure models

The importance of the different source terms can be evaluated based on their relative contribution to the flow field. The terms of major importance are the blade forces and the Reynolds stress (Simon 2007), the circumferential and unsteady stresses having a lower influence. Finally, the aperiodic stress is often neglected if the operating conditions are stable. On the other hand, it should be included if mistuning ought to be analysed. In the present case, the aperiodic and unsteady stresses are neglected since the results comparison is based on steady periodic RANS computations with uniform boundary conditions, in which these stresses vanish due to the underlying assumptions. Note that the neglected stresses correspond to error sources in RANS prediction[1]. Finally, the circumferential stress is also neglected.

The Reynolds stress is closed by the $k-l$ Smith model (Smith 1994). Strictly speaking, the turbulence model should be averaged in time, from passage-to-passage and circumferentially according to the Adamzcyk's cascade. However, RANS turbulence models are already based upon rather strong assumptions and the use of a turbulence model "as is" provides reasonable results. It resolves the boundary layer on the annulus endwalls and allows capturing the high flow gradient in these regions. The inviscid blade force $\mathbf{S_{bi}}$ is split into two contributions based on the blade surface description using the camber line cl and blade thickness $t(s)$ distributions. The resulting two terms $\mathbf{S_{bi_1}}$ and $\mathbf{S_{bi_2}}$ represent the effect of the blade blockage and the flow deflection in the blade row passage, respectively. However, the inviscid blade force contributions and the viscous blade force require the value of the pressure and shear stress on both sides of the blade, which is unfortunately unknown due to the axisymmetric assumption. Therefore, the blade forces have to be approximated from known averaged quantities.

For the blade blockage force, the average of the lower and upper blade surface pressure coming into play in the force expression is assumed to be equal to the averaged pressure p computed by the through-flow solver and

$$\mathbf{S_{bi1}} = \left[0, \frac{p}{b}\frac{\partial b}{\partial x}, \frac{p}{b}\frac{\partial b}{\partial r}, 0, 0\right]^T. \tag{2}$$

Note that only a circumferential blockage factor is incorporated. The second part of the inviscid blade force and the viscous blade force are modelled through body forces as

$$\mathbf{S_{bi2}} = [0 \quad f_{b,x} \quad f_{b,r} \quad f_{b,\theta} \quad f_{b,\theta}\Omega r]^T \quad \text{and} \quad \mathbf{S_{bv}} = [0 \quad f_{v,x} \quad f_{v,r} \quad f_{v,\theta} \quad f_{v,\theta}\Omega r]^T, \tag{3}$$

[1]The use of RANS simulations for result comparison is questionable as the reliability is still low according to the Adamczyk's cascade. However, these simulations are widely used in industry because higher levels of fidelity are almost inaccessible during the design process in view of their computational cost. RANS is thus considered the highest level of reliability used for design. Additionally, the reference simulations have been calibrated to best fit the test bench experimental results. Hence we do not need to outperform RANS and therefore it is most relevant to compare TF simulations to RANS rather than to more precise simulations such as LES.

where Ω is the rotation velocity of the shaft. The blade deflection force $\boldsymbol{f_b}$ is assumed to be perpendicular to the mean flow surface through the orthogonality condition

$$\boldsymbol{f_b} \cdot (\boldsymbol{V} - \Omega r \mathbf{e}_\theta) = 0, \tag{4}$$

where $\boldsymbol{V}$ and $\mathbf{e}_\theta$ are the velocity vector in the absolute frame of reference and the unit vector in the circumferential direction. This body force is intended to produce flow turning without any generation of work in the relative frame of reference and thus, without generating entropy. Additionally, the blade force magnitude is determined by assuming that the meridional stream surface followed by the flow is given by the mean-flow-path represented by the mean surface of the blade modified by some deviation angle δ. This deviation angle accounts for the fact that the actual flow does not exactly follow the camber line because of the presence of the blade boundary layer. It is formally defined as the local difference between the flow angle β and the blade (camber line) angle κ so that $\delta = \beta - \kappa$ along the chord. A time-marching procedure is used to enforce this slip condition, where the blade force modulus is modified by a quantity proportional to the orthogonality error between the blade force and the actual computed flow directions. This methodology has been applied by Baralon et al. (1998) and Pacciani et al. (2016) to the circumferential component of the force but it has been shown by Simon (2007) that the approach is less robust than applying it to the modulus of the blade force. Moreover, the force is directly imposed to be perpendicular to the mean-flow-path rather than to the mean flow surface during the iterative process. This methodology is more robust since the direction of the blade force does not fluctuate during the convergence process, as shown by Budo et al. (2021). At convergence the mean-flow-path coincides with the meridional stream surface. Finally, the components of the force are obtained by projecting the modulus onto the components normal to the flow direction.

Losses result from viscous blade forces and are introduced through a distributed loss model. The dissipative force is assumed to be aligned with the flow and pointing in the opposite direction, so that it only results in entropy generation. Using Crocco's equation, the corresponding entropy production is related to the dissipative force $\boldsymbol{f_v}$ as

$$f_v = \rho T \frac{W_m}{W} \partial_m s \quad \text{and} \quad \partial_m s = \frac{\Delta s_m}{l_m}, \tag{5}$$

where ρ, T, W and W_m are the density, the temperature, the velocity and the meridional velocity in the relative frame of reference, and the entropy gradient $\partial_m s$ is computed from an entropy jump across blade rows along meridional streamlines. Equation 5 is formally valid for an inviscid flow but it can be extended to viscous flow keeping the modeling error small. Finally, the entropy jump Δs_m is related to a loss coefficient through

$$\Delta s_m = c_p \log \frac{T_{t,\mathrm{TE}}}{T_{t,\mathrm{LE}}} - R \log \frac{p_{t,\mathrm{TE}}}{p_{t,\mathrm{LE}}}, \tag{6}$$

where c_p and R are the specific heat coefficient at constant pressure and the ideal gas constant, respectively. The total temperature ratio is computed from the rothalpy conservation while the total pressure ratio is expressed using the definition of the loss coefficient ω as

$$\frac{p_{t,\mathrm{TE}}}{p_{t,\mathrm{LE}}} = \frac{p_{t,is,\mathrm{LE}}}{p_{t,\mathrm{LE}}} - \omega \left(1 - \frac{p_{\mathrm{LE}}}{p_{t,\mathrm{LE}}} \right), \tag{7}$$

where $p_{t,is}$ is the isentropic total pressure. Finally, the unknown deviation angle δ and loss coefficient ω appearing in the blade forces are still unknown. The computation of these key parameters through correlations is further discussed in subsequent sections.

Numerical implementation

The system of governing equations is solved using a time-marching methodology. The left-hand side of Eq. 1 is computed by `elsA` using a finite volume formulation on structured meshes. The mesh is clustered in the endwall regions to accurately compute the boundary layer and at the blade leading and trailing edge to accurately capture the strong gradients there. The Reynolds stress and the miscellaneous source terms are also handled by `elsA`. Finally, the blade forces and the blade blockage terms are computed by `ASTEC` routines. The through-flow solver inherits its numerical scheme from the CFD software `elsA`. A backward Euler scheme with relaxation is used for the time discretization. Artificial dissipation is added with Jameson's scheme (Jameson et al. 1981). The convective fluxes are discretized using the Roe's second order upwind scheme. A multigrid approach is employed to speed up convergence to the steady state solution.

For boundary conditions, span-wise distributions of total pressure, total temperature and flow angles are imposed in the rotating frame of reference at the subsonic inlet. At the outlet, the static pressure is prescribed on a point of reference, and the radial equilibrium equation is used to compute the static pressure distribution. A no-slip condition is enforced at the endwalls (hub and casing). Finally, periodic boundary conditions are imposed on left and right surfaces of the single pitch-wise mesh cell due to the axisymmetric flow assumption.

Solver assessment

To validate the solver, through-flow simulations of a modern low-pressure compressor designed by Safran Aero Boosters are compared to the corresponding RANS simulations with a mixing plane approach using `elsA`. This highly loaded compressor features a high Mach number, but still subsonic, flow and its endwalls undergo an important radius variation. It is composed of three stages of 3D modern blades between an inlet guide vane (IGV) and a strut, as depicted in Fig. 1. The mesh is composed of about 40,000 cells. Simulations have been run for several values of the outlet pressure at nominal speed using a valve law to predict the performance for a set of mass-flow rates. The TF simulations are fed with the exact radial distribution of the key parameters δ_{TE} and ω from the corresponding high-fidelity computations in order to isolate the modeling error from correlation empiricism. The deviation angle δ is usually defined at the blade trailing edge but it is used here for the entire blade surface to account for the boundary layer on the blade wall. To obtain the deviation angle field δ, its radial distribution δ_{TE} at the trailing edge is linearly distributed on the entire blade along streamlines according to the local camber. At the LE, the deviation angle is thus equal to 0. The loss coefficient is kept constant along streamlines as it is computed from blade LE and TE positions. Through this analysis, we assess the through-flow model with respect to its underlying assumptions prior to evaluate its ability to predict geometric variability effects.

The comparison of compressor performance, evaluated with respect to the first row inlet and last row outlet stations, is shown in Fig. 1. The results are non-dimensionalized by reference values related to the operating conditions for confidentiality reasons. The through-flow simulations give accurate results along the overall performance curves while such a model is usually used to predict only nominal conditions at early design iterations. The mean epistemic error margin based on a L2 norm is around 2% and the run time of the throughflow simulation is at least two orders of magnitude lower than the corresponding RANS simulation. The relative difference for the total pressure ratio slightly increases as the mass-flow rate increases. This small disagreement between the performance predictions are mainly due to the circumferential stress that is intrinsically included in the RANS computations but neglected by the through-flow model. Moreover, rotor tip clearance and leakage flow cavity are currently not represented in the through-flow path. Their impact is only partially included in the prescribed parameters distribution. Discrepancy can also arise because of the difference in the turbulence models used by both simulations. Finally, a more realistic streamwise distribution of the key parameters δ_{TE} and ω could also improve the prediction, as shown by

Pacciani et al. (2016).

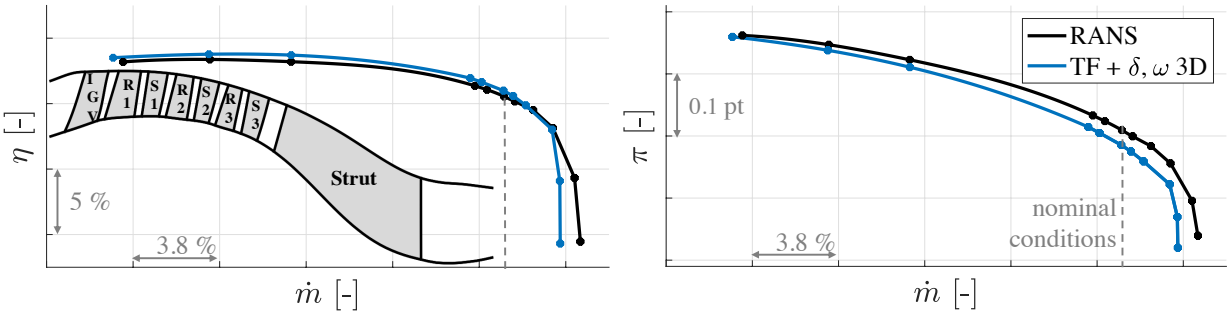

Figure 1: **Isentropic efficiency η (left) and total pressure ratio π (right) at the nominal rotational speed and meridional sketch of the compressor (left). Comparison of RANS and through-flow simulations fed with exact correlation parameters from RANS computations.**

At low mass-flow rate, the performance characteristics are limited by the non-convergence of both computational codes close to the same (numerical) stall onset point. The through-flow model is also able to predict accurately the maximum efficiency peak. However, at high mass-flow rate, the choking condition is achieved for a slightly lower mass-flow rate than RANS prediction. As explained by Baralon et al. (1998) and Simon (2007), a circumferential blockage, although consistent with the averaged governing equations, can lead to a poor quality of the solution in the analysis mode when the performance is sought knowing the real geometry. An alternative formulation called "normal" blockage proposed in place of the circumferential one and computed with respect to the stream-wise direction in the blade-to-blade plane should be implemented to improve the captured choking mass-flow rate. As a conclusion, it has been shown that the through-flow model is able to reproduce fairly well the 3D steady averaged flow field under the aforementioned assumptions provided that the key parameter distributions are precisely known (e.g., from high-fidelity data).

Correlations

The radial distribution of the deviation angle and loss coefficient is usually unknown, and are therefore obtained from empirical correlations. However, correlations adapted for modern engine designs, i.e., with highly loaded three-dimensional blades, are often kept confidential. As a consequence, the span-wise profiles of δ_{TE} and ω are computed here using empirical correlations developed by Lieblein (1960) and reported by Aungier (2003),

$$\delta_{\text{TE}}(r) = \delta^*_{\text{TE}} + \left[\frac{\partial\delta}{\partial i}\right]^* (i - i^*) + 10\left(1 - \frac{W_{m,\text{TE}}}{W_{m,\text{LE}}}\right) \quad \text{and} \quad \omega(r) = 2\frac{\theta_w(D_{eq})}{c}\frac{\sigma}{\cos\beta_{\text{LE}}}\left(\frac{W_{\text{TE}}}{W_{\text{LE}}}\right)^2, \quad (8)$$

where i is the incidence angle, c the blade chord length, σ the solidity and θ_w the wake momentum thickness, which is computed as a quadratic function of the equivalent diffusion factor D_{eq}. The latter depends on the difference between the actual and the optimal incidence angle, $i - i^*$. For the deviation angle, the contribution at design conditions corresponds to the first term on the right-hand-side of Eq. 8(a) and is based on Carter's rule (Carter 1950). The second term, representing the off-design contribution, is obtained using the methodology of Johnsen & Bullock (1965) and Pollard & Gostelow (1967), assuming a linear dependence on the incidence angle. The third term represents the dependence of the deviation angle on the axial velocity-density ratio (AVDR). For the loss coefficient, both design and off-design parts are included in the expression for θ_w. Finally, a third correlation is used to compute the optimal incidence angle i^*, i.e., the incidence angle that achieves minimal loss (Aungier 2003). More details can be found in the aforementioned

references. Note that these correlations only account for two-dimensional profile losses generated in a blade-to-blade plane. Budo et al. (2021) previously assessed their reliability on the CME2 compressor stage. TF predictions showed a global good agreement over the full operating range. An example of the streamline computed by the through-flow solver is reported in Fig. 2, which clearly illustrates the flow turning achieved by the blade forces in both blade rows. Moreover, the endwall boundary layers are well represented in the stream surface, as such a viscous formulation, unlike inviscid through-flow models, allows resolving the boundary layers on the annulus endwalls.

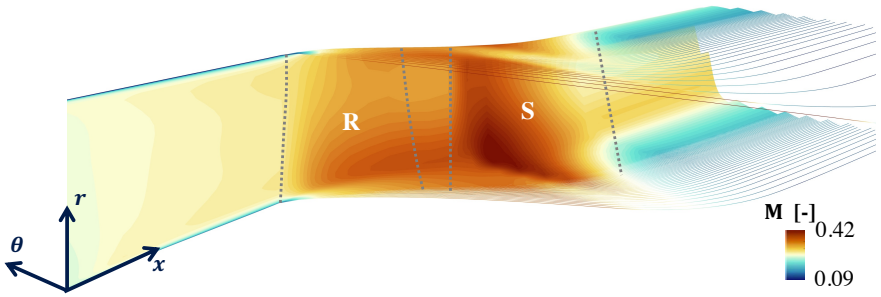

Figure 2: **Axisymmetric averaged stream lines for CME2 stage in nominal regime** ($\dot{m} = 10.5$ **kg/s), Mach number contours and fictitious position of rotor (R) and stator (S) blades.**

However, the adequacy of these correlations was previously shown to be poor when applied to the modern compressor (Budo et al. 2021). As illustrated in Fig. 3, the through-flow prediction represented by the purple line shows significant underpumping compared to RANS. This phenomenon can be explained by the overestimation of the deviation angle at the rotor trailing edge, as highlighted in the right part of Fig. 3 where the deviation angle law is plotted with respect to the incidence i. Therefore, modifications of the correlations have been introduced in order to improve the prediction. Specifically, the dominant terms of the deviation angle correlation, that is the slope parameter coming from Carter's rule (Carter 1950) has been modified. Moreover, Mach number effect, based on the work of Kónig et al. (1994), has been introduced in the loss coefficient correlation because some underestimation of the loss had been noticed in the Lieblein's correlation (Budo et al. 2021). As a result, the TF predictions (orange line in Fig. 3) are drastically improved and the performance curves show a satisfactory agreement. Although the agreement can be considered reasonable, the correlations should still be improved as the loss coefficient is under-estimated at negative stall incidence. Moreover, the linear law predicted by the deviation angle correlation reproduces fairly well the deviation angle behavior in a range relatively close to the optimal incidence angle i^*, i.e., the incidence angle that achieved minimal loss, but completely fails to predict off-design conditions. As a conclusion, the reliability of the through-flow results depends mostly on the accuracy of the deviation and loss models and their span-wise distribution.

EVALUATION OF THE EFFECT OF GEOMETRIC VARIABILITY AT LEADING EDGE

Incidence correction

Although a satisfactory agreement is obtained between TF and RANS predictions, two additional modeling aspects that may impact the propagation of geometric variabilities at the blade leading edge, must be taken into account. The first one is related to the axisymmetric assumption and the analysis mode: for a given flow incidence, the flow direction at the blade row inlet does not follow the camber line at the leading edge. However, the flow angle in the bladed region is imposed by the blade flow deflection force in the analysis mode. Consequently, a discontinuity occurs at the leading edge. This discontinuity leads to a sudden and non-physical increase of entropy and a spurious generation of losses, as shown in Fig. 4. A numerical treatment is thus adopted to remove

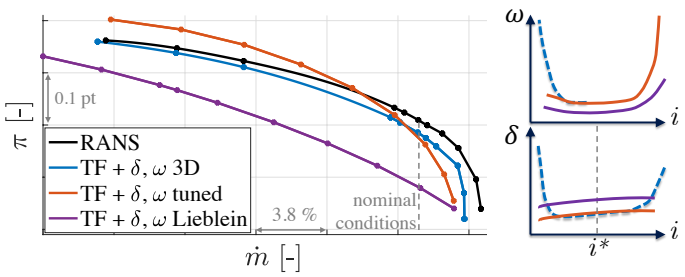

Figure 3: **Total pressure ratio as a function of the mass flow rate at the nominal rotational speed of the compressor (left). Comparison of RANS and through-flow simulations with different computed key parameters. Qualitative behavior of the key parameters δ and ω laws with respect to incidence (right).**

the flow discontinuity. The methodology consists in linearly modifying the mean-flow-path angle in the blade leading edge regions so that it adapts to the incident flow (Baralon et al. 1998).

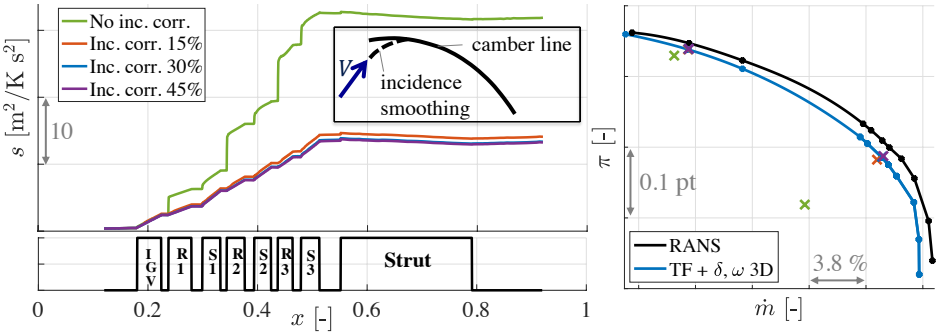

Figure 4: **Entropy generation due to leading edge discontinuity for different extents of the incidence smoothing and sketch of the smoothed blade geometry (left). Corresponding total pressure ratio (point data) at the nominal regime and maximum peak efficiency (right).**

As shown in the figure, the fix is applied so that the stream surface modification due to incidence affects the first few percents of the blade chord. The blade geometry is thus locally modified by this numerical artifact. In the present work, a smoothing on the first 30% of the chord is used unless otherwise specified. A smaller chord portion leads to entropy generation and performance mis-prediction while a longer portion impacts the geometry in a too large proportion. Even if this optimal choice introduces a low error in the global blade loading compared to the gain brought by a more physical behaviour of the loss generation, this modification of the blade geometry can also smooth any geometric variability in this region. A special attention should therefore be paid to this numerical artifact when propagating geometric uncertainties.

Camber line computation

The second aspect concerns the pre-processing of the blade geometry for TF simulations. Using prescribed velocity distribution design approaches, new highly optimized airfoils have been developed. Unlike NACA airfoils which are parameterized based on a known line of mean camber, modern airfoils are directly described by the position of the pressure and suction surface. However, TF simulations require a blade definition in terms of a mean camber line and a thickness distribution for the blade force computation. Therefore, the blade section outline must be split into mean camber line and thickness distribution. In the vicinity of the leading edge, and trailing edge to a lesser extent, algorithms determining a mean camber line can be unreliable because the line of camber is no longer quasi-parallel with the section outline (Lange et al. 2009) and its definition

is thereby not unique. As shown in the left part of Fig. 5, the blade angle κ can vary from 1 to 4 degrees close to the leading edge depending of the preprocessing tool. Although these tools are based on the same methodology, the LE treatment lead to dissimilar blade angle distributions, which may not be consistent with the blade loading distribution. The impact of this variability is relatively small, especially because the affected region is quite limited. Nonetheless, this epistemic uncertainty can exceed geometric variability in the leading edge region.

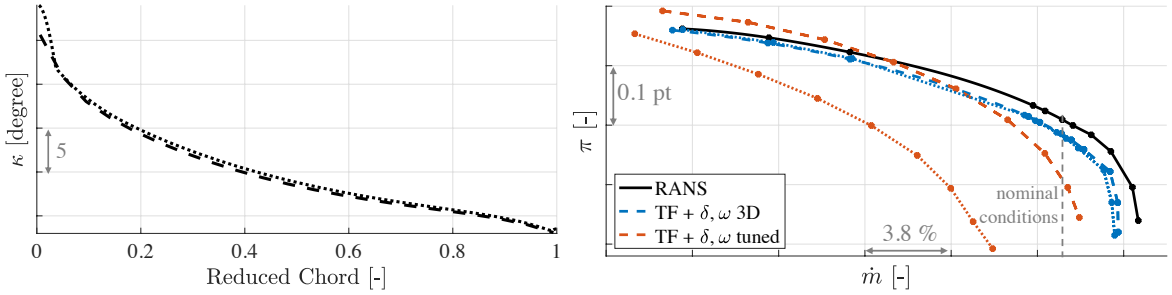

Figure 5: **Blade angle distribution along the chord (left) and total pressure ratio as a function of the mass flow rate (right) at the nominal rotational speed of the compressor for two airfoil splitting algorithms (dotted and dashed lines). Comparison of RANS and through-flow simulations with different computed key parameters (blue and orange lines).**

In order to assess the model sensitivity with respect to this uncertainty, TF simulations have been run based on the blade geometric outputs from two algorithms. The blade leading edge of each blade row computed by both algorithms varies from 1 to 4 degrees with respect to each other close to the leading edge. As shown in the right part of Fig. 5, the direct impact of the blade angle distribution (blue lines) is low on the blade force if the correlation parameters δ and ω are known, i.e., taken from the RANS simulations here. Since the incidence correction smears the leading edge uncertainty, the predictions of the TF simulations are quite similar for the two blade angle distributions of Fig. 5(left). As proposed by Pacciani et al. (2016), alternative smoothing formulations should be considered to decrease the leading edge stiffness. However, the empirical correlations for δ, ω and, especially i^*, use the actual geometry as input and are highly sensitive to the LE and TE blade angle. As a result, the blade angle uncertainty indirectly influences the blade forces through these correlations. It can be seen that, in this case, the TF model (orange lines in Fig. 5(right)) demonstrates a large variability in its prediction. The methodology adopted here to alleviate this uncertainty consists in using the value of the blade angle outside the uncertainty region, i.e., at a few percents of the chord further downstream, as input for the calibrated correlations. The performance thus obtained corresponds to the orange line in Fig. 3. An alternative solution could consist in extending the camber line in the region of interest according to a linear or higher order law, consistently with the blade loading.

Leading edge blade angle effects

In this section, the model ability to capture geometric variability effects on the compressor performance is assessed at nominal conditions. As a preliminary analysis, only the blade leading edge is modified by $\pm 1.5°$ over the first 20% of the chord along the blade span. A comparison between TF and steady RANS simulations is presented hereafter. For each simulation, only one blade row is modified. The comparison of compressor performance variation with respect to TF and RANS baseline simulations, respectively, is shown in Fig. 6. As explained above, a blade geometry modification at the leading edge is mainly felt through the correlations for δ and ω. As a result, the model is able to predict performance variation with respect to this geometric variability. The global trend is well captured by the TF model. However, the relative performance variation

is largely overestimated by the TF solver, meaning that the epistemic uncertainty stemming from the aforementioned aspects has a large contribution in this case. Nevertheless, these results are a promising first step towards the use of such TF model for industrial design and the efficient evaluation of other types of blade geometric variabilities.

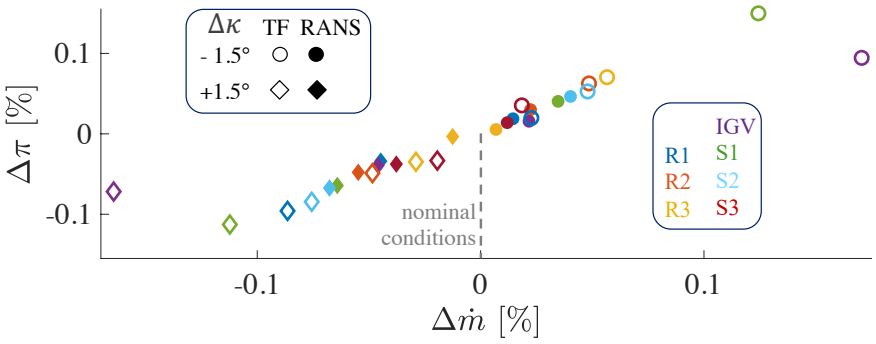

Figure 6: **Changes in pressure ratio and mass flow rate due to LE blade angle κ variation. Comparison of RANS and TF simulations for which each time a single blade row is modified.**

CONCLUSION

This paper presents the evaluation of a viscous CFD-based through-flow solver and its adequacy to predict geometric variability effects on compressor performance. A modern highly loaded multi-stage axial low-pressure compressor designed by Safran Aero Boosters is used as a test-case to assess the reliability of the method. It has been shown that the distribution of the key parameters δ and ω is critical as a good prediction of them provides a very good match between RANS and TF, as shown by a priori tests using RANS input data. But the improved empirical correlations for these two parameters are still not very accurate, leading to non-negligible discrepancies between RANS and TF simulations. The propagation, and thus the evaluation, of geometric uncertainties is marred by additional epistemic uncertainties inherent to the TF model. Moreover, the incidence correction needed to mitigate the spurious entropy increase at the blade leading edge and the camber line computation have a significant impact on the performance prediction. The former tend to smooth any geometric variability in this region. The latter has a significant impact on the deviation angle and loss coefficient predicted by the empirical correlations. Hence, strategies have been proposed to mitigate these model uncertainties. However, if these parameters are correctly predicted (i.e., here from RANS simulations), discrepancies with respect to RANS become very small. Finally, a preliminary study indicates that the TF model is able to partly capture the effect of geometric changes of the blade leading edge but the epistemic uncertainty stemming from the aforementioned aspects has a large contribution in this case. The results are promising and future work should assess the model prediction with respect to other types of blade deformation. Note that, due to the axisymmetry assumption on which the TF model is based, as the periodicity of the simulations of reference (RANS), geometric variabilities are intrinsically identical on each blade of the row, which is incompatible with mistuned blade row analysis. Nevertheless, the relevance of the present study is motivated by the analysis of recurring deformation patterns linked to tolerances and the blade manufacturing process. Mistuned blade rows would be tackled by such an axisymmetric approach though, averaging the blade row geometries.

ACKNOWLEDMENTS

This work is jointly funded by the Walloon region, under grant no. 7900, and Safran Aero Boosters in the frame of the project MARIETTA. The authors are also very thankful to Safran Aero Boosters for sharing data, and to Safran Tech and Onera for providing the softwares.

REFERENCES

Adamczyk, J. J. (1984), Model equation for simulating flows in multistage turbomachinery.

Aungier, R. H. (2003), *Axial-Flow Compressors*.

Baralon, S., Erikson, L.-E. & Hall, U. (1998), Validation of a throughflow time-marching finite-volume solver for transonic compressors, *in* 'Proceedings of the ASME Turbo Expo'.

Budo, A., Terrapon, V. E., Arnst, M., Hillewaert, K., Mouriaux, S., Rodriguez, B. & Bartholet, J. (2021), Application of a viscous through-flow model to a modern axial low-pressure compressor, Vol. 2A: Turbomachinery — Axial Flow Fan and Compressor Aerodynamics of *Turbo Expo: Power for Land, Sea, and Air*.

Carter, A. (1950), The Low Speed Performance Of Related Aerofoils In Cascades.

Föllner, S., Amedick, V., Bonhoff, B., Brillert, D. & Benra, F.-K. (2020), Model validation of an euler-based 2D-throughflow approach for multistage axial turbine analysis, *in* 'Proceedings of the ASME Turbo Expo', Vol. 29, pp. 185–186.

Jameson, A., Schmidt, W. & Turkel, E. (1981), Numerical solution of the euler equations by finite volume methods using runge kutta time stepping schemes, *in* '14th Fluid and Plasma Dynamics Conference'.

Jian, L., Dongrun, W., Jinfang, T., Mingmin, Z. & Xiaoqing, Q. (2020), The effects of incidence and deviation on the CFD-based throughflow analysis, *in* 'Proceedings of the ASME Turbo Expo', number 14293, pp. 1–9.

Johnsen, I. & Bullock, R. (1965), *Aerodynamic Design of Axial-Flow Compressors*, number SP-36.

Kónig, W. M., Hennecke, D. K. & Fottner, L. (1994), 'Improved Blade Profile Loss And Deviation Angle Models For Advanced Transonic Compressor Bladings: Part I - A Model For Subsonic Flow', *ASME Journal of Turbomachinery* **118**(1), 73–80.

Lange, A., Vogeler, K., Gümmer, V., Schrapp, H. & Clemen, C. (2009), Introduction of a parameter based compressor blade model for considering measured geometry uncertainties in numerical simulation, *in* 'ASME Journal of Turbomachinery', number 59937, pp. 1–11.

Lange, A., Voigt, M., Vogeler, K., Johann, E., Royce, R., Kg, C. & Dahlewitz, D. (2012), Principal component analysis on 3D scanned compressor blades for probabilistic CFD simulation, *in* 'Proceedings of the AIIA Conference', number 1762, pp. 1–16.

Lieblein, S. (1960), 'Incidence and Deviation-Angle Correlations for Compressor Cascades', *ASME Journal of Turbomachinery* **82**(3), 575–584.

Nigro, R. (2018), Uncertainty Quantification for Robust Design of Axial Compressors, PhD thesis.

Pacciani, R., Rubechini, F., Marconcini, M., Arnone, A., Cecchi, S. & Daccà, F. (2016), 'A CFD-based throughflow method with an explicit body force model and an adaptive formulation for the S2 streamsurface', *Proceedings of the Institution of Mechanical Engineers, Part A: Journal of Power and Energy* **230**(1), 16–28.

Pollard, D. & Gostelow, J. P. (1967), 'Some Experiments at Low Speed on Compressor Cascades', *Journal of Engineering for Gas Turbines and Power* **89**(3), 427–436.

Righi, M., Pachidis, V., Könözsy, L. & Pawsey, L. (2018), 'Three-dimensional through-flow modelling of axial flow compressor rotating stall and surge', *Aerospace Science and Technology* **78**, 271–279.

Simon, J.-F. (2007), Contribution to Throughflow Modelling for Axial Flow Turbomachines, PhD thesis.

Smith, B. R. (1994), A Near Wall Model for The k-l Two Equation Turbulence Model, *in* 'Proceedings of the AIIA Conference', number 2386, pp. 1–8.

Wu, C.-H. (1952), A general theory of three-dimesional flow in subsonic and supersonic turbomachines of axial-, radial-, and mixed-flow types, Technical report, NACA.